Applied Acoustics 103 (2016) 71–81

Contents lists available at ScienceDirect

Applied Acoustics

journal homepage: www.elsevier.com/locate/apacoust

Optimal acoustic design of multi-source industrial buildings by means of a simplified acoustic diffusion model

Martín E. Sequeira [1], Víctor H. Cortínez *

Centro de Investigaciones en Mecánica Teórica y Aplicada, Facultad Regional Bahía Blanca, Universidad Tecnológica Nacional, 11 de Abril 461, B8000LMI Bahía Blanca, Argentina

ARTICLE INFO

Article history:
Received 29 May 2015
Received in revised form 10 August 2015
Accepted 9 October 2015

Keywords:
Optimal design
Two-dimensional acoustic diffusion model
Simulated Annealing algorithm
Passive treatments

ABSTRACT

Noise in industrial workplaces has become an important occupational problem. Accordingly, there is a need to implement cost-effective strategies for reducing noise levels.

In this paper, an optimal design methodology of passive acoustic treatments is proposed with the objective of minimizing the corresponding economic cost while keeping noise levels below tolerant limits. The methodology is based on a combination of a recently developed simplified acoustic diffusion model with a stochastic optimization technique known as "Simulated Annealing". The simplified diffusion model allows one to accurately evaluate multiple acoustic situations with a low computational cost, and the Simulated Annealing method is used to direct the search of the optimum set of design variables.

Some numerical examples are presented in order to show the effectiveness of the proposed approach.

1. Introduction

Industrial noise associated with production processes has become an important occupational problem. In fact, remaining in excessively noisy environments for long periods may cause workers significant hearing damage as well as psychological disorders [1]. For that reason, noise regulations are becoming more restrictive, setting lower exposure limits in noisy environments as well as maximum tolerable level values in industrial buildings. The most widely used form of noise reduction is passive control. In particular, the use of multi-layer sound absorbers on the interior surfaces to reduce reverberant sound field, and/or the implementation of acoustical enclosures to reduce direct noise radiated by machinery, can constitute a simple, reliable and durable solution. The economic cost associated with these sound treatments depends on the quality of the acoustic materials and the application surface. Therefore, it is necessary to design them carefully and efficiently in order to reduce the high cost involved.

The more convenient treatment configurations may be obtained by means of exhaustive simulations involving variations of the acoustic parameters. In these simulations, one needs to predict noise levels generated in the analyzed room for several values of the characteristics of the absorbers and the enclosures, such as application surfaces and internal architecture of the panels. The successive design trials will be acceptable if the maximum noise levels are lower than established limits. The best option corresponds to the less expensive of these feasible possibilities. This trial and error practice is, in general, very time consuming. In order to facilitate this task, it is possible to employ an optimal design method. This last one constitutes an automatic procedure that minimizes the number of necessary simulations in order to find the best solution.

In this paper, an optimal design methodology of the passive acoustic treatments previously mentioned is proposed with the objective of minimizing the corresponding economic cost while keeping noise levels below tolerant limits. The methodology is based on a combination of a stochastic optimization technique known as "Simulated Annealing algorithm" [2] and a recently developed simplified acoustic diffusion model SADM [3,4].

It is necessary to employ an optimization method, for directing the search of the optimum set of design variables, with a reduction in the number of simulations required for calculating the corresponding objective function and constraints. There exist classical well-known methodologies based on gradient descent [5]. However, these ones require the objective function to be continuous and convex with respect to the design variables. This is not the case for the present problem. For this reason, stochastic methods are preferred. In particular, the selected Simulated Annealing (SA) technique is suitable for analyzing optimization problems with discrete variables and with many local optima [6,7].

* Corresponding author. Tel.: +54 0291 4555220; fax: +54 0291 4555311.
E-mail addresses: martins@frbb.utn.edu.ar (M.E. Sequeira), vcortine@frbb.utn.edu.ar (V.H. Cortínez).
[1] Tel.: +54 0291 4555220; fax: +54 0291 4555311.

http://dx.doi.org/10.1016/j.apacoust.2015.10.005
0003-682X/

Even so, in the optimization process, it is highly desirable the use of an acoustic prediction model sufficiently accurate and computationally fast to estimate the effects (noise levels) of different technical alternatives, because the simulations should be performed many times. In this connection, the simplified diffusion model (SADM) is proposed for evaluating the constraints of the problem because it allows one to accurately evaluate multiple acoustic situations with a low computational cost [4,8]. This method is a simplification of the acoustic diffusion model ADM, first proposed by Ollendorff [9] and later developed by Picaut et al. [10], that allows one to predict the sound field in non-uniform reverberant conditions. This last one constitutes a crucial improvement of the classical Sabinés theory. In general, the ADM shows an accuracy comparable to that given by classical geometrical acoustic models [3,4,11–19].

In Section 2, the optimal design problem is formulated. In Section 3, the simplified diffusion model is presented along with embedded formulations for the multi-layer sound absorber and the acoustical enclosure. In Section 4, the use of the Simulated Annealing technique for directing the search of the optimum design is described. In Section 5, numerical examples are given to show the efficiency of the proposed methodology. Finally, in Section 6 the main conclusions are presented.

2. Problem formulation

It is considered the situation of an industrial workroom with multiple acoustic sources (machineries) emitting constant sound powers along the working day. In order to reduce the noise levels, two types of technical solutions are selected: multi-layer sound absorbers, to mitigate the reverberant sound field and acoustical enclosures with interior sound absorbing treatments, to insulate the sound sources.

The adopted multi-layer absorber is composed of a perforated plate backed by a porous material, an air cavity and a rigid wall (Fig. 1). This configuration improves the acoustic performance in relation to a single porous material and allows to extend the absorption frequency range. The absorption of this kind of device is characterized by means of its absorption coefficient, which is determined as a function of the following design variables: the thickness t_a of the air cavity, the thickness t_m of the porous material, the porosity ξ of the perforated plate and the diameter d of the perforated holes.

For the case of the acoustical enclosure of a source, the sound insulating quality is determined by the insertion loss IL, which is defined as a function of the following design variables: the average energy absorption coefficient $\bar{\alpha}_E$ and the sound transmission loss TL_E.

The aim of the design approach is to minimize an objective function OF that represents the total economic cost of the adopted solutions, while keeping the noise levels below a tolerant limit. Accordingly, the optimization problem is formulated as follows

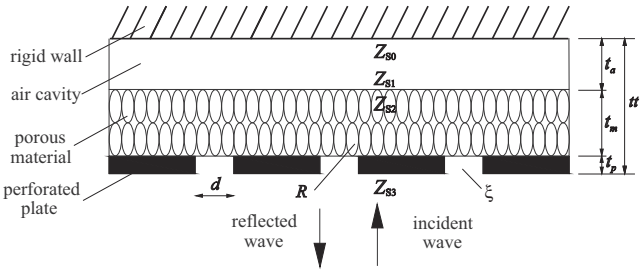

Fig. 1. Scheme of the selected multi-layer sound absorber configuration.

$$(t_a, t_m, \xi, d, \bar{\alpha}_E, TL_E)_{opt} = \text{argmin} OF, \tag{1}$$

where $(\ldots)_{opt}$indicates the set of the optimal design variables. The economic cost (OF) is defined as

$$OF(t_a, t_m, \xi, d, \bar{\alpha}_E, TL_E) = \sum_{i=1}^{N} C_i \times S_{S,i} + \sum_{o=1}^{M} \bar{C}_o \times S_{E,o}, \tag{2}$$

being N the number of interior surfaces i to be acoustically treated; C_i represents the economic cost per unit area of the acoustic absorber to treat the surface i, which depends on the thickness of the absorbent material t_m; $S_{S,i}$ is the area of the surface i; M is the number of sources o; $\bar{C}_o$ represents the cost per unit area of the acoustical enclosure to treat the source o, which depends on the average energy absorption coefficient $^{-}{}_E$ and the sound transmission loss TL_E of the selected enclosure and $S_{E,o}$ is the interior wall surface of the enclosure to treat source o.

The minimization of the objective function OF is associated with two types of restrictions. First, the total thickness of the multi-layer absorbers is constrained to 0.16 m. This is a physical restriction that takes into account the necessity of access and maintenance. This limit value is only illustrative and it can change depending on the particular situation [6].

On the other hand, to protect workers from the presence of occupational noise exposure, a permissible level is set as the quantity that must not be exceeded along the working day. Accordingly, the overall sound pressure A-weighted level SPL_A is assumed to be limited to 85 dBA. This acoustical restriction is based on the current labor legislation in Argentine that imposes an equivalent sound exposure level of 85 dBA as the daily permissible noise level [20].

Therefore, the OF minimization is subject to the following restrictions

$$tt = t_a + t_m + t_p \leq 0.16 \text{ m}, \tag{3}$$

$$\text{SPL}_\text{A}(\mathbf{r}) \leq 85 \text{ dBA}, \tag{4}$$

where tt is the total thickness of the multi-layer absorber and t_p is the thickness of the perforated plate. In particular, $\text{SPL}_\text{A}(\mathbf{r})$ depends on the receiver position $\mathbf{r} = (x, y, z)$, the sound power level contribution of every source and the selected design variables. The explicit mathematical expression for $\text{SPL}_\text{A}(\mathbf{r})$ is shown in the following section.

3. Acoustic models

In order to estimate the sound levels, the acoustic diffusion model is used. For this task, it is necessary to account for the source power levels and the acoustic properties of the selected sound treatments, characterized by the absorption coefficients of the multi-layer absorbers and the sound insertion losses of the acoustical enclosures. These acoustic parameters depend directly on the design variables previously presented and they are obtained by means of two proposed sub-models. In this section, such models are described.

3.1. Sound propagation model

3.1.1. Acoustic diffusion model

This model allows to simulate the non-uniform reverberant sound field in rooms based on an analogy with particles propagation in a dispersive medium. Accordingly, it is assumed that the density dispersion is large and the energy reflection is dominant over absorption. Hence, reflections in the interior surfaces and objects within the room are supposed diffusive and the energy flow and density variations are considered small [10]. Following this

assumptions, the stationary sound energy density $w_f(\mathbf{r})$ corresponding to the reverberant field, at location $\mathbf{r}$ for the frequency f and in a room of volume V_r, is obtained as the solution of the following governing system [3,14]

$$D\nabla^2 w_f(\mathbf{r}) - \sigma_f w_f(\mathbf{r}) + q_f(\mathbf{r}) = 0 \text{ in } V_r, \tag{5}$$

$$D\frac{\partial w_f(\mathbf{r})}{\partial \mathbf{n}} + A_f c w_f(\mathbf{r}) = 0 \text{ on } \partial V_r, \tag{6}$$

where ∇^2 is the Laplace operator, D is a diffusion coefficient, σ_f is a term that account for the volumetric absorption, $q_f(\mathbf{r})$ is the source sound power per unit volume, $\mathbf{n}$ is the exterior normal to the boundaries, A_f is the absorption factor of the interior surfaces and c is the speed of sound. The diffusion coefficient D can be expressed as [3,11]

$$D = \begin{cases} \frac{c\lambda_r}{3} \times K & \text{for empty rooms,} \\ \frac{c\lambda_r\lambda_{fitt}}{3(\lambda_r+\lambda_{fitt})} \times K & \text{for fitted rooms.} \end{cases} \tag{7}$$

For empty rooms, D considers the morphology of the room with interior surfaces area S_r through the respective mean free path $\lambda_r = 4V_r/S_r$. If a sub-volume V_{fitt} of V_r contains scatter objects (*fittings*), the diffusion is described by the mean path length for a sound ray between two collisions with an object $\lambda_{fitt} = 4/(S_{fitt}\, n_{fitt})$, where S_{fitt} represents the surface area of the object and n_{fitt} is the number of scattering objects per unit volume in V_{fitt}. Thus, the diffusion coefficient D for fitted rooms is obtained from a combination of the diffusely-reflecting surfaces of the room and the scattering obstacles within the room [11]. The function $K = -2.238\ln(s) + 1.549$ allows to include mixed specular and diffuse reflections on room boundaries, being s the scattering coefficient of the surfaces [17]. This coefficient is used to determine the proportion of energy that is reflected in a specular manner and the proportion that is scattered [21]. Values for the scattering coefficient s can spread out over the range from 0 (completely specular reflections) to 1 (completely diffuse reflections). In particular, the law of the function K is valid for $10^{-3} \leqslant s < 1$ and for $s = 1$, $K = 1$ [11,17].

On the other hand, coupled rooms are configurations typically found in industrial buildings. Several enclosures are coupled when they are connected through open surfaces, which allow transmission of sound energy from one space to another. In these cases, it must be obtained one value for the coefficient D for each sub-volume as a function of its geometric dimensions [12].

The absorption term σ_f is given by the following expressions

$$\sigma_f = \begin{cases} m_f c & \text{for empty rooms,} \\ m_f c + \frac{c\alpha_{S_{\text{fitt}},f}}{\lambda_{\text{fitt}}} & \text{for fitted rooms.} \end{cases} \tag{8}$$

In empty rooms, this term takes into account the atmospheric attenuation, being m_f the coefficient of atmospheric attenuation in m^{-1} [15]. In fitted rooms, it is obtained from the sum of the absorption contribution of the air and the fittings, respectively, being $\alpha_{S,fitt,f}$ the absorption coefficient of the obstacles located into the room [11].

Expression (6) corresponds to the boundary conditions on interior surfaces. The absorption factor A_f depends on the absorption coefficient $\alpha_{S,f}$ of the considered surface [3,13,14]. In this paper, the absorption factor proposed by Jing and Xiang [14] is used. This factor allows one to characterize the absorption over the entire range of application and it is expressed as follows

$$A_f = \frac{\alpha_{S,f}}{2(2-\alpha_{S,f})}. \tag{9}$$

The sound pressure A-weighted level $\text{SPL}_{A,f}$ is determined by adding the contributions of direct and reverberant sound fields [3,11]

$$\text{SPL}_{A,f}(\mathbf{r}) = 10\log_{10}\left\{\rho c\left[\int_{V_S}\frac{q_f(\mathbf{r})}{4\pi r^2}\exp\left(-\frac{r}{\lambda_{\text{fitt}}}\right)\text{d}V_S + \text{cw}_f(\mathbf{r})\right]\Big/P_{\text{ref}}^2\right\} + \text{PondA}, \tag{10}$$

where PondA is the A-weighted function [22], $r = \|\mathbf{r} - \mathbf{r_s}\|$ denotes the distance from a receiver point to an arbitrary point of the source $\mathbf{r_s}$ in the subdomain V_S, ρ is the air density and $P_{\text{ref}} = 2 \times 10^{-5}$ Pa. Only point sources with in-time constant sound powers are considered, so the source term is written as

$$q_f(\mathbf{r}) = \sum_{o=1}^{M}\overline{W}s_{\text{fo}}\delta(\mathbf{r}-\mathbf{r}_{\mathbf{s},o}) = \sum_{o=1}^{M}\left[10^{(\text{SWL}_{\text{fo}}-IL_{\text{fo}})/10}\times W_0\right]\delta(\mathbf{r}-\mathbf{r}_{\mathbf{s},o}), \tag{11}$$

where SWL_{fo} is the sound power level of the source o for the frequency f, IL_{fo} is the insertion loss of the acoustical enclosure

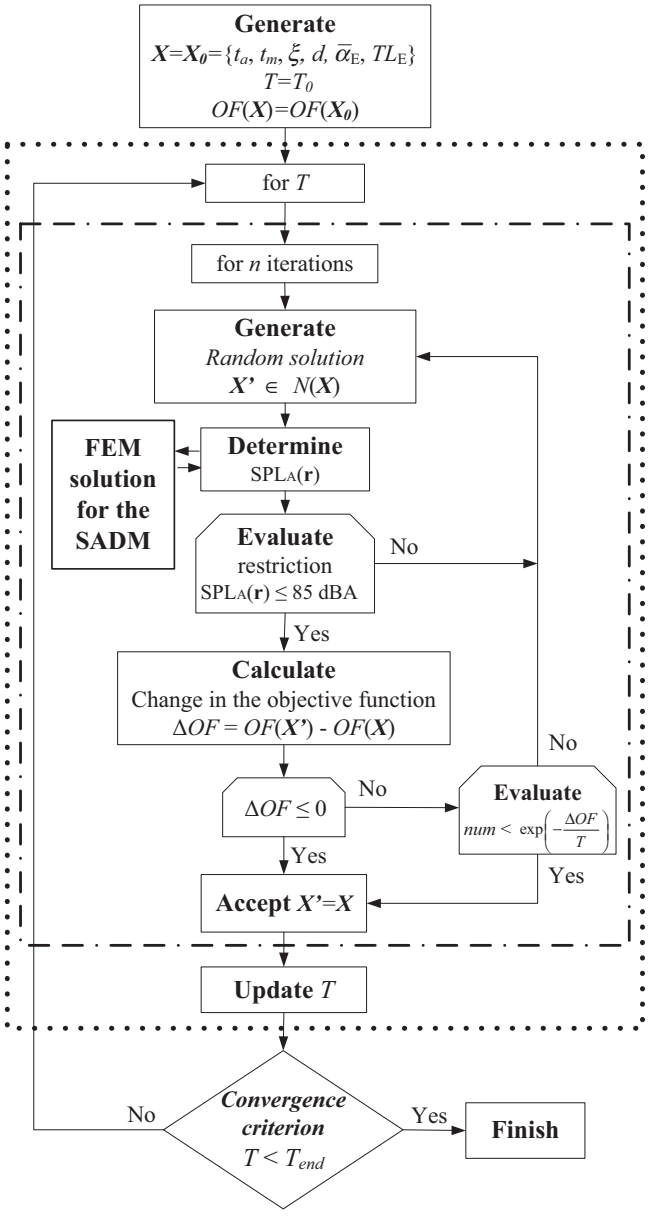

Fig. 2. Flowchart of the Simulated Annealing algorithm.

to mitigate the source o, $\overline{W}s_{fo}$ is the sound power of the source o including the attenuation due to the enclosure (IL) and $W_0 = 10^{-12}$ W.

In this paper octave-frequency bands are considered, so the overall sound pressure A-weighted level SPL_A is written as

$$SPL_A(\mathbf{r}) = 10\log_{10}\left(\sum_{fb=1}^{Nfb} 10^{\frac{SPL_{A_{fb}}(\mathbf{r})}{10}}\right), \quad (12)$$

where fb is the octave-frequency band of interest and Nfb is the number of frequency bands selected.

Obviously, the idealization of real sources as emitting points is reasonable only when the machineries are of small dimensions in comparison with those of the workroom. This implies that the acoustic field very close to the point source is not real and it is not considered.

On the other hand, considering the fact that the sound sources are constant over time, the indicator SPL_A coincides with the equivalent steady noise level of a noise energy-averaged over time LAeq, which is the most widely used indicator in the majority of the noise regulations, particularly, in Argentine legislation [20].

3.1.2. Simplified acoustic diffusion model

The usual ceiling geometries of industrial workrooms correspond to flat surfaces at least in an approximated form. Taking advantage of this fact, the full acoustic diffusion model ADM may be approximately reduced to a simplified two-dimensional diffusion equation by means of the Kantorovich method [23]. This is a well-known technique for the dimensional reduction of differential equations that occupies an intermediate position, from a precision viewpoint, between the exact solution and the solution which is obtained by means of Ritz and Galerkin methods. Accordingly, the reverberant energy density $w_f(\mathbf{r})$, at location $\mathbf{r}$ for the frequency f, can be approximated by the product of two functions, one corresponding to the variation in the domain related to the horizontal plane and the other considering the variation in height. Thus, the reverberant energy density can be expressed as [4]

$$w_f(\mathbf{r}) \approx \tilde{w}_f(\mathbf{r}) = P_f(x,y) \times Z(z), \quad (13)$$

where $P(x, y)$ is an unknown function and $Z(z)$ is a function selected *a priori* in order to approximate the vertical variation of the reverberant energy density. This methodology presents the advantage that only part of the solution is chosen in advance, while the remainder thereof is determined according to the nature of the problem.

The simplest way to approximate the vertical variation of the reverberant energy density is by means of the second order polynomial $Z(z) = 1 + a_1 z + a_2 z^2$. The polynomial coefficients are

Table 1
Transmission loss values and economic costs of the insulating panels used in the enclosures.

Enclosure panel	Insulating quality	TL_E values (dB) by octave-frequency band				Economic cost ($) per unit area
		250 Hz	500 Hz	1000 Hz	2000 Hz	
20 g aluminum sheet, stiffened (0.9 mm thick)	A	10	10	18	23	10
22 g galvanized steel sheet (0.55 mm thick)	B	14	20	23	26	15
18 g galvanized steel sheet (1.2 mm thick)	C	20	24	29	33	20

Table 2
Absorption coefficients and economic costs of the material used in the enclosures.

Polyurethane foam (28 kg/m^3)	Absorbing quality	Absorption coefficient $\bar{\alpha}_E$ by octave-frequency band				Economic cost ($) per unit area
		250 Hz	500 Hz	1000 Hz	2000 Hz	
20 mm thick	A	0.1	0.32	0.5	0.57	5
35 mm thick	B	0.24	0.43	0.64	0.68	10
50 mm thick	C	0.38	0.7	0.91	0.76	15
75 mm thick	D	0.67	0.86	0.98	0.88	20

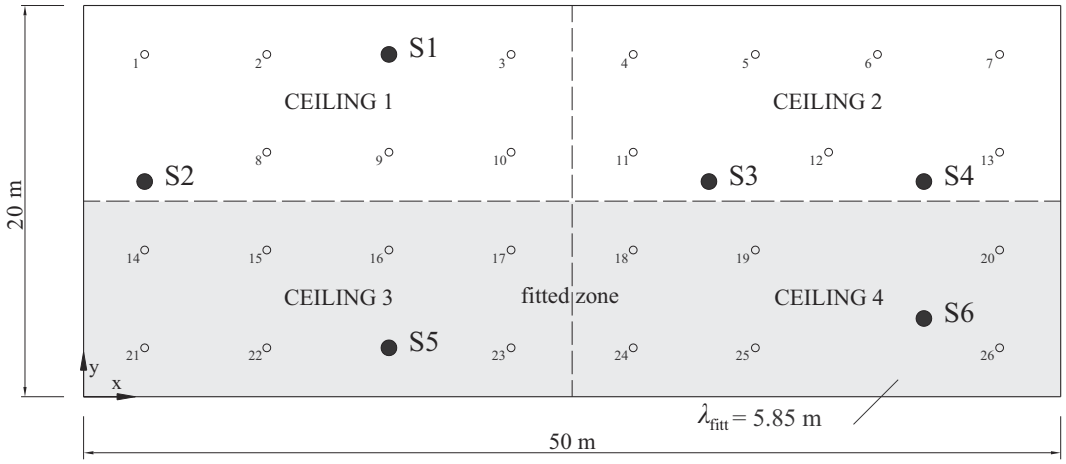

Fig. 3. Scheme of the fitted workroom with the locations of the sources (S) and the ceiling surfaces to be treated. The acoustic restriction ($SPL_A \leqslant 85$ dBA) is evaluated at the receiver points marked with (○).

determined from the boundary conditions defined in the two extreme planes of the room (floor and ceiling)

$$D\frac{dZ(z)}{dz} = \pm A_f Z(z). \tag{14}$$

According to the Kantorovich method [23], substituting the approximated expression (13) into Eqs. (5) and (6), multiplying by $Z(z)$ and integrating over the height H of the room, it is possible to arrive to the following system of equations corresponding to the simplified acoustic diffusion model SADM [4]

Table 3
Sound power levels and coordinates of the sources.

Sound source	Coordinate (m)		Sound power level (SWL, dB re 10^{-12} W) by octave-frequency band			
	x	y	250 Hz	500 Hz	1000 Hz	2000 Hz
S1	15.6	17.5	90	96	104	108
S2	3.1	11	91	93	95	102
S3	32	11	89	94	97	98
S4	43	11	95	100	106	106
S5	15.6	2.5	105	107	110	109
S6	43	4	109	110	106	106

Table 4
Comparison of SPL_A values at the receiver points in the fitted workroom. The values in parentheses are the variations against the SADM (units in dBA).

Point	1	2	3	4	5	6	7
SADM	89.3	92.4	92.2	88.4	88.5	90.4	90.9
ADM	89.3	92.4	92.2	88.4	88.5	90.4	90.9
	(0)	(0)	(0)	(0)	(0)	(0)	(0)
RT	88	89.9	89.3	86.9	87.6	90.4	89.8
	(1.3)	(2.5)	(2.9)	(1.5)	(0.9)	(0)	(1.1)
Point	8	9	10	11	12	13	14
SADM	91.7	93.8	91.1	89.4	92.4	93.5	90.5
ADM	91.7	93.8	91.1	89.3	92.4	93.5	90.5
	(0)	(0)	(0)	(0.1)	(0)	(0)	(0)
RT	89	92.3	88.4	86.9	90.7	91.8	89.3
	(2.7)	(1.5)	(2.7)	(2.5)	(1.7)	(1.7)	(1.2)
Point	15	16	17	18	19	20	21
SADM	92.6	96.1	92.3	88.9	90.8	95.2	88.4
ADM	92.5	96.2	92.3	88.8	90.7	95.2	88.3
	(0.1)	(−0.1)	(0)	(0.1)	(0.1)	(0)	(0.1)
RT	89.6	96	89.2	85.6	88.4	92.3	88.1
	(3)	(0.1)	(3.1)	(3.3)	(2.4)	(2.9)	(0.3)
Point	22	23	24	25	26		
SADM	94.9	94.9	88.1	90.5	96.4		
ADM	94.8	94.8	88.3	90.3	96.4		
	(0.1)	(0.1)	(−0.2)	(0.2)	(0)		
RT	93.9	93.5	86.1	87.4	93.4		
	(1)	(1.4)	(2)	(3.1)	(3)		

$$D_{Z1}\nabla_p^2 P_f(x,y) + (D_{Z2} - \sigma_{Z,f})P_f(x,y) + q_{Z,f} = 0 \text{ in } \Omega, \tag{15}$$

$$D_{Z1}\frac{\partial P_f(x,y)}{\partial \mathbf{n}} + A_{Z,f}cP_f(x,y) = 0 \text{ on } \partial\Omega, \tag{16}$$

where ∇_p^2 is the Laplace operator in the plane and Ω represents the domain of the horizontal plane (with perimeter $\partial\Omega$) of the considered room. From Eqs. (15) and (16) the following definitions have been made

$$D_{Z1} = \int_0^H DZ(z)^2 dz, \tag{17}$$

$$D_{Z2} = \int_0^H D\left(\frac{d^2Z(z)}{dz^2}Z(z)\right)dz, \tag{18}$$

$$\sigma_{Z,f} = \int_0^H \sigma_f Z(z)^2 dz, \tag{19}$$

$$q_{Z,f} = \int_0^H q_f Z(z) dz, \tag{20}$$

$$A_{Z,f} = \int_0^H A_f Z(z)^2 dz. \tag{21}$$

Once $P_f(x, y)$ is obtained as the solution of the previous system of equations, the approximated reverberant energy density is given by expression (13) and the overall sound pressure A-weighted level is obtained by means of expressions (10)–(12).

3.2. Multi-layer sound absorber model

The adopted absorber is composed of three layers: a perforated plate, a porous material and an air cavity backed by a rigid wall. The selected configuration is shown in Fig. 1. The surface impedance of the configuration is estimated by the transfer matrix method using the following relation [21,24]

$$Z_{S,k+1} = \frac{-jZ_{S,k}Z_k\cot(k_{c,k}t_k) + Z_k^2}{Z_{S,k} - jZ_k\cot(k_{c,k}t_k)}, \tag{22}$$

where $Z_{S,k+1}$ is the impedance of the bottom of layer $k+1$; $Z_{S,k}$ is the impedance of the bottom of layer k; $j = \sqrt{-1}$ and Z_k, $k_{c,k}$ and t_k are the characteristic impedance, the wavenumber and the thickness of layer k, respectively. This formulation is used recursively to successive layers in order to obtain the surface impedance of the multi-layer absorber.

Table 5
Results from the optimization approach in the fitted workroom.

Surface	Selected absorption coefficient α_S by octave-frequency band				Selected multi-layer absorber variable			
	250 Hz	500 Hz	1000 Hz	2000 Hz	t_a (m)	t_m (m)	ξ (%)	d (m)
Ceiling 1	0.02	0.03	0.03	0.04	–	–	–	–
Ceiling 2	0.02	0.03	0.03	0.04	–	–	–	–
Ceiling 3	0.03	0.14	0.64	0.56	0.02	0.01	10	0.006
Ceiling 4	0.02	0.03	0.03	0.04	–	–	–	–
Source	Selected insertion loss IL (dB) by octave-frequency band				Selected insulating/absorbing quality (see Tables 1 and 2)			
S1	0.22	4.83	13.74	17.43	A/A			
S2	0.22	4.83	13.74	17.43	A/A			
S3	0.22	4.83	13.74	17.43	A/A			
S4	8.04	9.12	16.66	19.32	A/D			
S5	3.46	13.21	16.86	18.64	B/A			
S6	13.95	18.78	21.43	21.18	C/C			

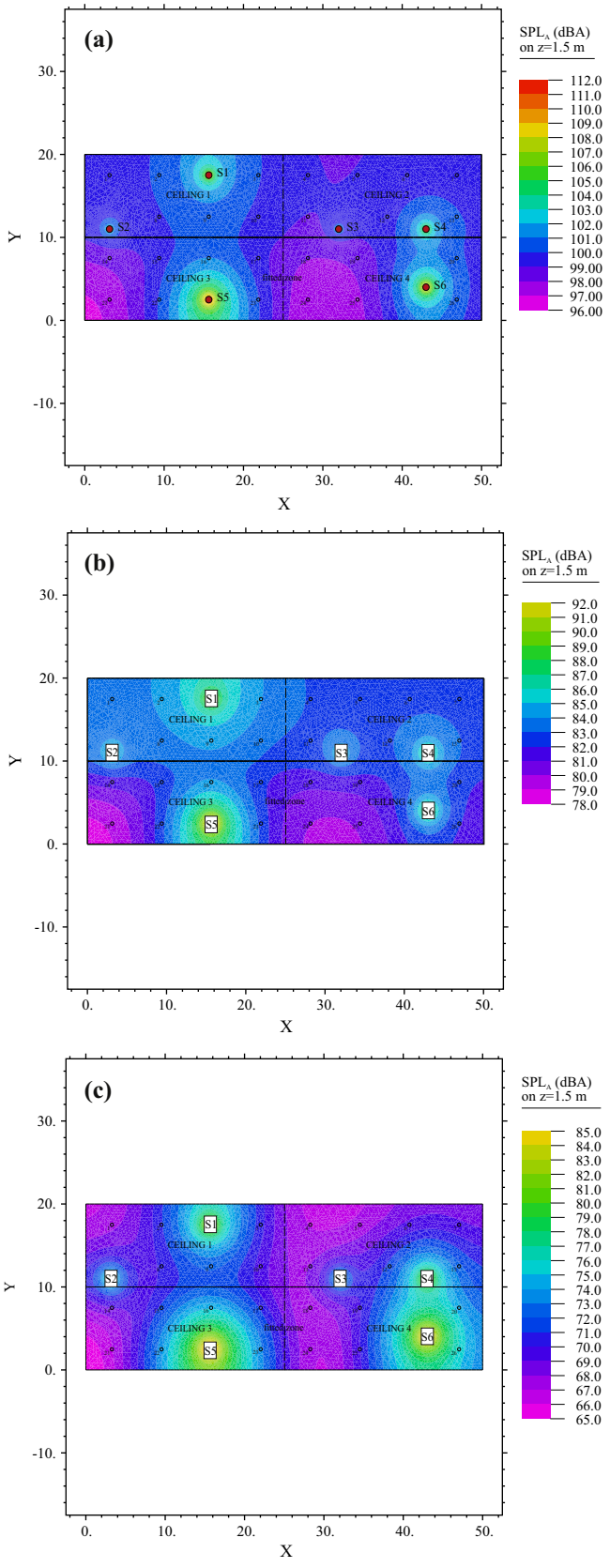

Fig. 4. SPL$_A$ distribution: without acoustic treatments (a), optimal acoustic treatments (b) and close to the best acoustic treatments (c).

From Eq. (22), the surface impedance of the air cavity with rigid backing is defined as

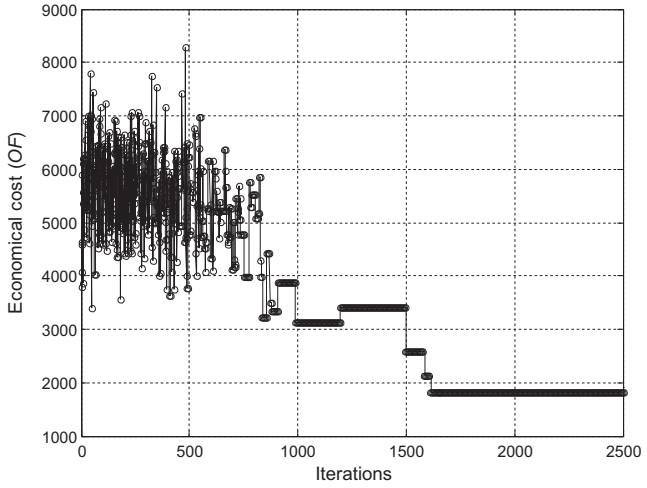

Fig. 5. Evolution of the objective function (economical cost) as a function of the number of iterations for the fitted workroom.

$$Z_{S1} = -\mathrm{j}Z_{S0}\cot(k_{c,a}t_a), \tag{23}$$

where $Z_{S0} = \rho c$ is the characteristic impedance of air and $k_{c,a} = \omega/c$ is the wavenumber of air, being $\omega = 2\pi f$. The surface impedance of the porous material mounted in front of the rigid wall with the air cavity is defined as

$$Z_{S2} = \frac{-\mathrm{j}Z_{S_1}Z_m\cot(k_{c,m}t_m) + Z_m^2}{Z_{S1} - \mathrm{j}Z_m\cot(k_{c,m}t_m)}, \tag{24}$$

where Z_m and $k_{c,m}$ represent the complex characteristic impedance and the complex wavenumber of the porous material, respectively. Those parameters are estimated from the semi-empirical formula for specific normal impedance developed by Delany and Bazley [25]. This formulation was obtained from the adjustment of several experimental data of wool materials through its specific airflow resistivity R in a certain frequency range and it is expressed as

$$\begin{cases} Z_m = Z_{S0}\left(1 + 0.05\Xi^{-0.754} - j0.087\Xi^{-0.732}\right), \\ k_{c,m} = \frac{\omega}{c}\left(1 + 0.0978\Xi^{-0.7} - j0.189\Xi^{-0.595}\right), \end{cases} \tag{25}$$

where $\Xi = \rho f/R$ is a dimensionless parameter.

The normal surface impedance of the perforated plate Z_p, in low-sound pressure level without mean flow, is estimated by the formula presented by Beranek and Ver [22]. The expression is defined as

$$\begin{cases} Z_p = \frac{\rho}{\xi}\sqrt{8\nu\omega}\left(1 + \frac{t_p}{d}\right) + j\frac{\omega\rho}{\xi}\left[\sqrt{\frac{8\nu}{\omega}}\left(1 + \frac{t_p}{d}\right) + t_p + \kappa\right], \\ \kappa = 0.85d\left[1 - 1.47(\xi)^{1/2} + 0.47(\xi)^{3/2}\right], \end{cases} \tag{26}$$

where ν is the kinematic velocity of air and κ is a correction factor that considers the edge of neck radiation impedance of the perforations. Then, the surface impedance of the multi-layer absorber is expressed as

$$Z_{S3} = Z_{S2} + Z_p. \tag{27}$$

Finally, the normal incident sound absorption coefficient is estimated as

$$\alpha_S(t_a, t_m, \xi, d, t_p, f, R) = 1 - \left|\frac{Z_{S3} - Z_{S0}}{Z_{S3} + Z_{S0}}\right|^2. \tag{28}$$

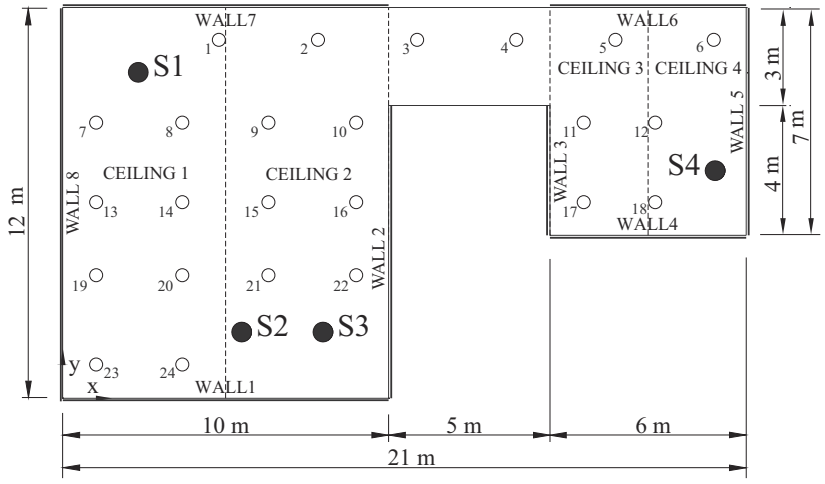

Fig. 6. Scheme of the coupled workroom with the locations of the sources (S) and the different surfaces (ceilings 1–4 and walls 1–8) to be treated. The acoustic restriction (SPL_A < 85 dBA) is evaluated at the receiver points marked with (○).

Table 6
Comparison of SPL_A values at the receiver points in the coupled workroom. The values in parentheses are the variations against the SADM (units in dBA).

Point	1	2	3	4	5	6
SADM	98.5	95.7	94.5	94.6	96.1	97.3
ADM	98.6	95.7	94.4	94.5	96.2	97.4
	(−0.1)	(0)	(0.1)	(0.1)	(−0.1)	(−0.1)
RT	97.2	94.9	93.7	94	95.9	97.9
	(1.3)	(0.8)	(0.8)	(0.6)	(0.2)	(−0.6)
Point	7	8	9	10	11	12
SADM	99.6	99.1	96.6	95.1	96.6	98.5
ADM	99.8	99.3	96.6	95.1	96.7	98.7
	(−0.2)	(−0.2)	(0)	(0)	(−0.1)	(−0.2)
RT	98.4	97.5	94.7	94.4	97.4	98.6
	(1.2)	(1.6)	(1.9)	(0.7)	(−0.8)	(−0.1)
Point	13	14	15	16	17	18
SADM	97.1	96.8	96	95.3	97.5	99.4
ADM	97.1	96.9	96.1	95.3	97.5	99.5
	(0)	(−0.1)	(−0.1)	(0)	(0)	(−0.1)
RT	95.9	95.4	94.3	94.5	97.7	99.5
	(1.2)	(1.4)	(1.7)	(0.8)	(−0.2)	(−0.1)
Point	19	20	21	22	23	24
SADM	95.8	96.2	96.6	95.9	95.1	96.1
ADM	95.8	96.3	96.7	96	95.1	96.2
	(0)	(−0.1)	(−0.1)	(−0.1)	(0)	(−0.1)
RT	94.8	94.7	95.2	95.1	94.3	95.3
	(1)	(1.5)	(1.4)	(0.8)	(0.8)	(0.8)

3.3. Acoustical enclosure model

Acoustical enclosures with interior sound absorbing treatments are considered. The performances of such enclosures are evaluated by means of the insertion loss *IL*. This indicator depends on multiple factors such as the sound transmission loss of each panel, the interior absorbing materials, the presence of leaks or/and openings, the coupling between the machine and interior walls and the flanking transmission through the floor and position of the machine. Here, *IL* is determined by the following analytical formula [22]

$$IL \cong 10\log_{10}\frac{S_E\bar{\alpha}_E}{\sum S_E \times 10^{-TL_E/10} + \sum S_L \times 10^{-TL_L/10}}, \tag{29}$$

where S_E is the interior wall surface of the enclosure and S_L and TL_L are, respectively, the area and the transmission loss of the leaks due to possible errors in the assembly and/or mounting conditions. In particular, S_L is adopted as 0.5% of the wall surface S_E. Expression (29) is valid if the following restriction is verified [26]

$$\frac{fV_E^{1/3}}{c} \geq 1, \tag{30}$$

where V_E is the enclosure volume.

It is important to note that during the simulations, the acoustical enclosures are considered as "fittings" and they are modeled in a statistical form [11]. It means that the exterior surfaces of the acoustical enclosures are not explicitly modeled and they are out of analysis. As it is mentioned in Section 3.1.1, only point sources with in-time constant sound powers are considered and the attenuation of the emitted power due to the enclosure is represented by means of a reduction (*IL*) in the original power of each one.

4. Numerical optimization model

4.1. Simulated Annealing method

The Simulated Annealing SA method is a heuristic combinatorial technique based on a random generation of feasible solutions whose main characteristic is to avoid local convergence in problems of great scale. The concept behind SA was developed by Kirkpatrick et al. [27]. The name of this method is derived from an analogy with a thermodynamic process of *annealing* where a metal is heated until a stabilization temperature is reached and then it is cooled slowly in order to achieve a thermal equilibrium characterized by a minimum-energy state. A controlled temperature decrease scheme prevents defects in the metal. This optimization routine allows determining quasi-optimal designs searching the best solution without the need of the correct choice of an initial search point as required by the gradient-based algorithms [28].

The algorithm starts by defining an initial solution $\boldsymbol{X_0}$ within the feasible region of the problem. Then, it successively generates, in a *reduced domain* $N(\boldsymbol{X})$ of the neighborhood of the actual solution, new solutions $\mathbf{X}'$ which are accepted as current according to the change in the objective function $\Delta OF = OF(\boldsymbol{X}') - OF(\boldsymbol{X})$. If this change is negative, the new solution will be admitted as the new current solution. If not, the acceptance of the increment will be calculated according with a probabilistic criterion defined as

$$\text{prob}(\Delta OF, T) = \exp\left(-\frac{\Delta OF}{T}\right) > num, \tag{31}$$

where T is a convergence parameter known as *temperature* (the name is derived from the physical analogy previously mentioned) and *num* is a random number in the interval [0, 1]. Therefore, configurations with a lower value of *OF* are accepted unconditionally while configurations with a greater value of *OF* are accepted more likely at the beginning, when the temperature is high, but as the process advances (and the temperature decreases), become less likely. Thus, SA allows accepting worse solutions than the current one in order to escape from the local optima. As the algorithm progresses, T is lowered so as to limit the probability of accepting feasible solutions that do not produce an improvement in *OF*.

The function that determines and controls the decrease of the temperature T plays a fundamental role in the efficiency of the algorithm. The selected scheme is defined as

$$T_{a+1} = \beta \times T_a, \tag{32}$$

where β is the *cooling rate* and, in general, $\beta \in [0.3, 0.999]$. Due to the stochastic nature of the SA method, the parameter β value is very problem-dependent [6,28]. Therefore, some calculations with different β values were performed in order to determine the most appropriate one to obtain a satisfactory solution for the present problem. After preliminary studies, a value of $\beta = 0.98$ is adopted.

In the early phase of the method, an initial temperature T_0 is defined. Then, the system progresses from one temperature T_a to another T_{a+1} when n number of iterations is completed. In order to accept all possible solutions with equal probability, T_0 must be high enough. A suitable expression for T_0 is given by [28]

$$T_0 = r_a \times \max \Delta \mathrm{OF}, \tag{33}$$

where r_a is a scalar value greater than 1. Finally, the process is repeated until T reaches a predefined end value defined as T_{end} (adopted convergence criterion).

4.2. Numerical implementation

The optimization methodology is implemented in Matlab. The absorption coefficients of the multi-layer absorbers and the insertion losses of the acoustical enclosures are estimated by means of the corresponding models described in Sections 3.2 and 3.3. The results are used to feed the SADM in order to obtain the sound field distribution. The SADM is solved by means of the Finite Element Method FEM implemented in the software Flex-PDE. The optimization process is determined from Matlab by linking the solutions of the SADM with the SA technique in an iterative manner. The flowchart of the general algorithm is showed in Fig. 2.

5. Numerical examples

Two configurations of typical industrial workrooms are selected. To perform the calculations the octave-frequency bands of 250, 500, 1000 and 2000 Hz are considered. The 250-Hz band is consistent with the lower frequency limit of application from the acoustic diffusion equations and the Delany and Bazley model [12,25].

For the acoustical enclosures, three different types of sound insulating panels and four different thicknesses of a sound absorbing material are chosen. Transmission loss values, absorbing material characteristics and economic costs per unit area are presented in Tables 1 and 2. The selected acoustic values are taken from materials commonly used in these cases [29,30]. The adopted costs are hypothetical and the $ symbol represents a non-defined monetary unit. The area of the interior wall surfaces for all possible enclosures is $S_E = 11.4\ \mathrm{m}^2$ ($2 \times 1.5 \times 1.2\ \mathrm{m}^3$). These dimensions are consistent with Eq. (30) for the lower band of interest (250 Hz).

For the multi-layer absorbers, the design variable values are: $0.01\ \mathrm{m} \leqslant t_a \leqslant 0.08\ \mathrm{m}$, $0.01\ \mathrm{m} \leqslant t_m \leqslant 0.145\ \mathrm{m}$, $10\% \leqslant \xi(\%) \leqslant 40\%$, $0.002\ \mathrm{m} \leqslant d \leqslant 0.008\ \mathrm{m}$, $t_p = 0.001\ \mathrm{m}$ and $R = 21{,}000$ Rayls/m (see expression (25)), which correspond to a mineral wool with a density of $100\ \mathrm{kg/m}^3$ [31]. The economic cost of the absorber is characterized by the thickness of the porous material (t_m) and it is expressed by the hypothetical formula $C = 44.45 \times t_m + 0.56$. This expression establishes a minimum cost per unit area $C(\min) = \$\ 1$ for $t_m(\min) = 0.01$ m and a maximum cost per unit area $C(\max) = \$\ 7$ for $t_m(\max) = 0.145$ m.

In the initial situation (before any acoustic treatments), the absorption coefficients of interior surfaces (smooth concrete) of the workrooms are: 0.02, 0.03, 0.03 and 0.04 for the octave frequency-bands of 250, 500, 1000 and 2000 Hz, respectively [32]. The atmospheric absorption coefficients considered are $m = 3 \times 10^{-4}$, 5×10^{-4}, 1×10^{-3}, $3 \times 10^{-3}\ \mathrm{m}^{-1}$ for the octave frequency-bands of 250, 500, 1000 and 2000 Hz, respectively.

For each example, in order to validate the proposed SADM, the corresponding $\mathrm{SPL_A}$ distribution is compared with the values determined by using the ADM and the Ray Tracing RT technique. This last one is obtained by using the software CATT-Acoustic™ v8.

Table 7
Results from the optimization approach in the coupled workroom.

Surface	Selected absorption coefficient α_S by octave-frequency band				Selected multi-layer absorber variable			
	250 Hz	500 Hz	1000 Hz	2000 Hz	t_a (m)	t_m (m)	ξ (%)	d (m)
Ceiling 1	0.02	0.03	0.03	0.04	–	–	–	–
Ceiling 2	0.59	0.94	0.92	0.89	0.07	0.03	27	0.0055
Ceiling 3	0.56	0.89	0.92	0.91	0.05	0.04	36	0.002
Ceiling 4	0.13	0.44	0.86	0.65	0.05	0.01	21	0.0025
Wall 1	0.02	0.03	0.03	0.04	–	–	–	–
Wall 2	0.02	0.03	0.03	0.04	–	–	–	–
Wall 3	0.49	0.93	0.91	0.72	0.075	0.02	12	0.002
Wall 4	0.35	0.84	0.96	0.78	0.045	0.025	13	0.0065
Wall 5	0.02	0.03	0.03	0.04	–	–	–	–
Wall 6	0.33	0.79	0.99	0.82	0.045	0.025	16	0.0025
Wall 7	0.74	0.84	0.84	0.96	0.075	0.06	40	0.006
Wall 8	0.02	0.03	0.03	0.04	–	–	–	–
Source	Selected insertion loss IL (dB) by octave-frequency band				Selected insulating/absorbing quality (see Tables 1 and 2)			
S1	0.22	4.83	13.74	17.43	A/A			
S2	3.58	6.11	14.81	18.20	A/B			
S3	0.22	4.83	13.74	17.43	A/A			
S4	0.22	4.83	13.74	17.43	A/A			

For the validation stage, no acoustic treatments are considered except on the ceiling surfaces where high-absorption absorbers are used. The adopted absorption coefficients are: 0.69, 0.8, 0.92 and 0.98 for the octave frequency-bands of 250, 500, 1000 and 2000 Hz, respectively. These values correspond to the following design variables: $t_a = 0.02$ m, $t_m = 0.12$ m, ξ (%) = 17% and $d = 0.002$ m. All the calculations were done in the same CPU.

5.1. Example 1: Workroom with a fitted zone

The 4-m high workroom shown in Fig. 3 is studied. A fitted zone of volume $50 \times 10 \times 4$ m^3 is considered. It is characterized by an objects density, uniformly distributed, of 0.171 l/m corresponding to $\lambda_{fitt} = 5.85$ m. The absorption coefficients of the fitted objects (industrial machinery) are set to 0.15, 0.15, 0.10 and 0.10 for the octave-frequency bands of 250, 500, 1000 and 2000, respectively [32]. Six omnidirectional point sources with a height of 1 m are contemplated. Their power levels and locations are presented in Table 3. The four ceiling surfaces and the six sources are considered to be acoustically treated (see Fig. 3). All the remaining surfaces are assumed without acoustic treatments. The reflections on the surfaces are considered completely diffuse.

Table 4 shows the comparison between the diffusion models and the Ray Tracing RT technique as a function of the SPL_A values at the receiver points, located at $z = 1.5$ m, shown in Fig. 3. A finite element mesh of about 1.7×10^3 triangular elements and 33×10^3 tetrahedral elements was used to solve the SADM and the ADM, respectively. The RT simulation was performed with 400×10^4 sound rays (for each source) and the fitted zone was simulated with 80 rectangular blocks ($0.75 \times 0.75 \times 4$ m^3) distributed uniformly with a mean path length equal to that adopted in the diffusion models ($\lambda_{fitt} = 5.85$ m).

The validation results demonstrate that the SADM practically coincides with the ADM and presents a mean error (maximum error) of 1.8 dBA (3.3 dBA) with respect to the RT simulation. The employed computation time is of the order of 2 s for the SADM, 90 s for the ADM and 43,000 s (~12 h) for the RT model.

Optimization results are presented in Table 5. Fig. 4a and b show the SPL_A distribution without and with the optimal acoustic treatments, respectively. It is noted that once implemented the optimal treatments, the SPL_A is lower than 85 dBA at the receiver points (see Fig. 4b). In addition, Fig. 4c shows the SPL_A distribution corresponding to treatments close to the best from the acoustical point of view. Obviously, this situation corresponds to a high-cost solution. The selected treatments consider high-absorption absorbers on the ceiling surfaces (with absorption coefficients equal to those used in the validation stage) and the highest insulating and absorbing qualities for all the acoustical enclosures (see Tables 1 and 2).

The evolution of the objective function is shown in Fig. 5. By around of 1700 iterations the optimal solution is reached with an economic cost $OF = \$\ 1811.4$. The close to the best solution presents an $OF = \$\ 7616$. It is observed that the economic cost variation between the optimal configuration and the better one is significant and it is of the order of 75%. Moreover, it is interesting to mention that the optimization process presents a computation time of about 11 h, while the computation time for the same process using the ADM would be of the order of 490 h.

5.2. Example 2: Coupled workroom

A 5-m height workroom consisting of three interconnected spaces is presented in Fig. 6. The main building contains three sound sources and is connected through a corridor to a second building with another source. The corridor is mixed specularly and diffusively reflecting (scattering coefficient $s = 0.3$) while the remaining spaces are completely diffusively reflecting.

The omnidirectional point sources are: source 1 (S1) at position ($x = 2.3$ m, $y = 10$ m and $z = 1$ m), source 2 (S2) at position

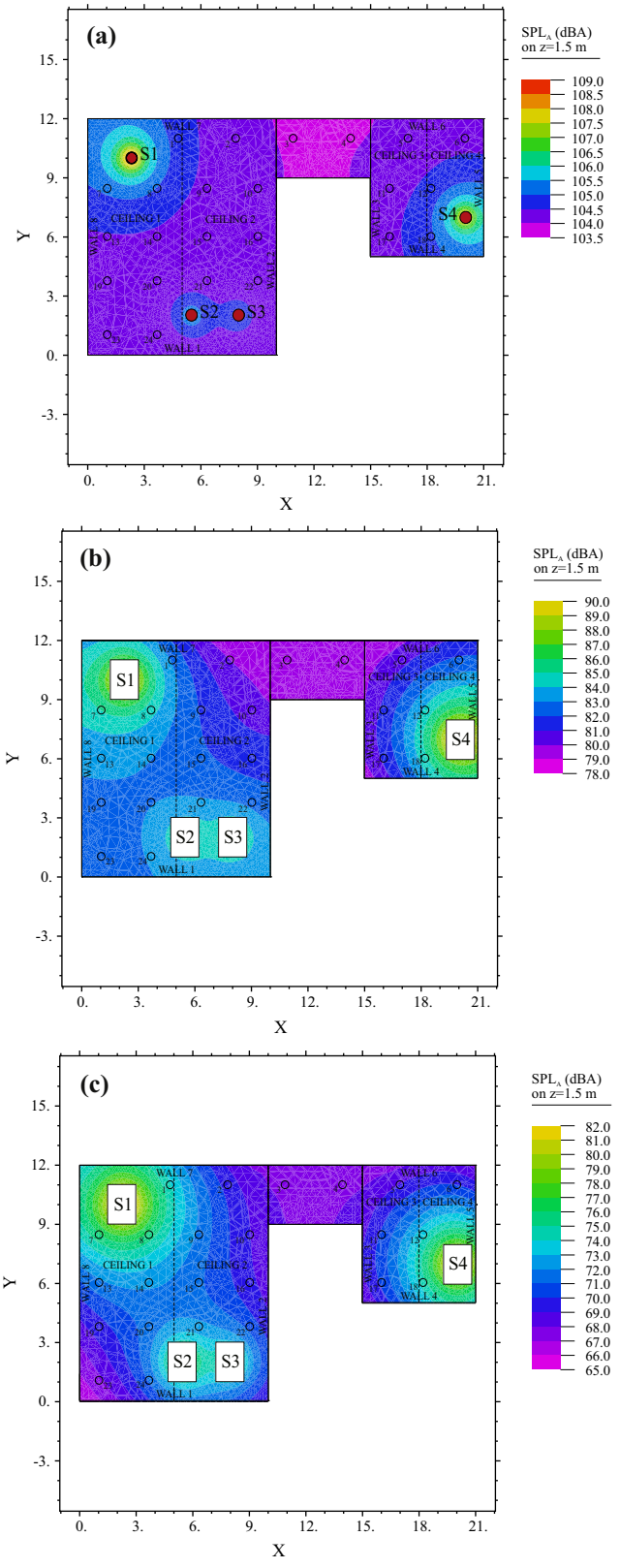

Fig. 7. SPL_A distribution: without acoustic treatments (a), optimal acoustic treatments (b) and close to the best acoustic treatments (c).

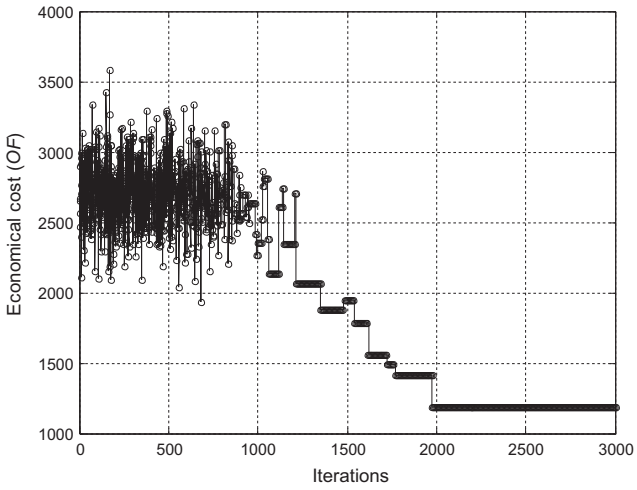

Fig. 8. Evolution of the objective function (economical cost) as a function of the number of iterations for the coupled workroom.

($x = 5.5$ m, $y = 2$ m and $z = 1$ m), source 3 (S3) at position ($x = 8$ m, $y = 2$ m and $z = 1$ m) and source 4 (S4) at position ($x = 20$ m, $y = 7$ m and $z = 1$ m). The sound powers are the same shown in Table 3. Four ceiling surfaces (ceilings 1–4), eight wall surfaces (walls 1–8) and the four sources are considered to be acoustically treated (see Fig. 6). The rest of the surfaces (the ceiling and the walls of the corridor) are not treated.

Comparison between the diffusion models and the RT technique, as a function of the SPL_A at the receiver points on a plane at $z = 1.5$ m, is shown in Table 6. A finite element mesh of about 8×10^2 triangular elements and 17×10^3 tetrahedral elements was used to solve the SADM and the ADM, respectively. The RT simulation was performed with 10×10^4 sound rays (for each source).

The validation results evidence a close fit between the SADM and the ADM and a good agreement with the RT simulation with a mean error (maximum error) of 1 dBA (1.9 dBA), respectively. The employed computation time is of the order of 1.5 s for the SADM, 70 s for the ADM and 950 s for the RT model.

Optimization results are presented in Table 7. As in the previous example, Fig. 7a and b show the SPL_A distribution without and with the optimal acoustic treatments, respectively. Once implemented the optimal ones, the overall noise levels do not exceed the maximum value of 85 dBA at the receiver points (see Fig. 7b). Fig. 7c presents the SPL_A distribution corresponding to treatments close to the best from the acoustical point of view.

The evolution of the objective function is shown in Fig. 8. The optimal solution ($OF = \$\ 1213.5$) is reached around of 2100 iterations with a calculation time of about 5.5 h. The better solution presents an $OF = \$\ 3344$. The economic cost variation between the optimal configuration and the better one is of the order of 63%. Furthermore, the use of the ADM would enlarge the execution time in more than 250 h.

6. Conclusions

An optimization approach for the acoustic design in multi-source industrial buildings has been formulated. The objective of the design was the minimization of the economic cost corresponding to passive treatments limiting the noise levels below a certain tolerable value. Multi-layer sound absorbers on the surfaces were considered, for mitigating the reverberant sound field, along with acoustical enclosures to reduce the direct noise from the sources.

The absorption properties of the sound absorbers have been obtained by the transfer matrix method while the insertion loss has been estimated by an analytical formula for acoustically lined enclosures. The simplified diffusion model (SADM) has been proposed in order to estimate the sound field distribution. Hence, the optimal design formulation has been satisfactorily solved by the combined employment of the Simulated Annealing algorithm and the finite element solution of the SADM.

It has been demonstrated that the use of the proposed SADM improves the speed of convergence while maintaining practically the same accuracy than the ADM. From the examples presented, the computing times employed by the SADM are at least 40 times lesser than those required for the application of the ADM. This fact represents an important advantage in the context of optimal design proposed because of the necessity to estimate the sound field distribution for a large number of configurations and for each octave-frequency band of interest.

Of course, as final step, the obtained design solution may be revised taking advantage of a more accurate prediction model such as the ray tracing technique.

The presented methodology was approached to small sources. However, if sources (or the corresponding isolating enclosures) are of dimensions comparable to those of the workroom, the modification in the calculation domain should be taken into account and the inner acoustic field corresponding to the enclosure must be obtained in order to estimate the distribution of radiation of its surfaces. This fact will be analyzed in a future research.

Acknowledgements

The authors would like to thank the support of Secretaría de Ciencia y Tecnología of Universidad Tecnológica Nacional, Universidad Nacional del Sur (UNS) and CONICET. This work is part of the Doctoral thesis of M.E. Sequeira, at Department of Engineering of UNS.

References

[1] Nelson DI, Nelson RY, Concha-Barrientos M, Fingerhut M. The global burden of occupational noise-induced hearing loss. Am J Ind Med 2005;48:446–58.
[2] Rao SS. Engineering optimization: theory and practice. New Age International; 1996.
[3] Valeau V, Picaut J, Hodgson M. On the use of a diffusion equation for room-acoustic prediction. J Acoust Soc Am 2006;119:1504–13.
[4] Sequeira ME, Cortínez VH. A simplified two-dimensional acoustic diffusion model for predicting sound levels in enclosures. Appl Acoust 2012;73(8):842–8.
[5] Cappelli D'Orazio M, Fontana DM. Optimization of the acoustical absorption characteristics of an enclosure. Appl Acoust 1999;57(2):139–62.
[6] Chang YC, Yeh LJ, Chiu MC. Optimization of constrained composite absorbers using simulated annealing. Appl Acoust 2005;66(3):341–52.
[7] Ruiz H, Cobo P, Jacobsen F. Optimization of multiple-layer microperforated panels by simulated annealing. Appl Acoust 2011;72(10):772–6.
[8] Sequeira ME. Optimal acoustic re-design of industrial buildings. Doctoral thesis. Bahía Blanca, Argentina: Department of Engineering, Universidad Nacional del Sur; 2014 (in Spanish).
[9] Ollendorff F. Statistical room-acoustics as a problem of diffusion: a proposal. Acustica 1969;21(4):236–45.
[10] Picaut J, Simon L, Polack JD. A mathematical model of diffuse sound field based on a diffusion equation. Acta Acust United Acust 1997;83:614–21.
[11] Valeau V, Hodgson M, Picaut J. A diffusion-based analogy for the prediction of sound fields in fitted rooms. Acta Acust United Acust 2007;93:94–105.
[12] Billon A, Valeau V, Sakout A, Picaut J. On the use of a diffusion model for acoustically coupled rooms. J Acoust Soc Am 2006;120:2043–54.
[13] Billon A, Picaut J, Sakout A. Prediction of the reverberation time in high absorbent room using a modified-diffusion model. Appl Acoust 2008;69(1):68–74.
[14] Jing Y, Xiang N. On boundary conditions for the diffusion equation in room-acoustic prediction: theory, simulations and experiments. J Acoust Soc Am 2008;123(1):145–53.
[15] Billon A, Picaut J, Foy C, Valeau V, Sakout A. Introducing atmospheric attenuation within a diffusion model for room-acoustic predictions. J Acoust Soc Am 2008;123(6):4040–3.

[16] Xiang N, Jing Y, Bockman AC. Investigation of acoustically coupled enclosures using a diffusion-equation model. J Acoust Soc Am 2009;126(3):1187–98.
[17] Foy C, Valeau V, Billon A, Picaut J, Sakout A. An empirical diffusion model for acoustic prediction in rooms with mixed specular and diffuse reflections. Acta Acust United Acust 2009;95(1):97–105.
[18] Cortínez VH, Sequeira ME. Diseño acústico óptimo en recintos industriales basado en un modelo de difusión. Primeras Jornadas Regionales de Acústica – AdAA, Rosario, Argentina; 2009.
[19] Billon A, Picaut J, Valeau V, Sakout A. Acoustic predictions in industrial spaces using a diffusion model. Adv Acoust Vib 2012 260394.
[20] National Law N° 19,587/1972. "Health and Safety at Work" with its regulatory decree N° 351/1979 and resolution N° 295/03 amending decree 351/1979. Argentine (in Spanish).
[21] Cox TJ, D'Antonio P. Acoustic absorbers and diffusers: theory design and application. 2nd ed. Taylor & Francis; 2009.
[22] Vér IL, Beranek LL. Noise and vibration control engineering: principles and applications. 2nd ed. New York: Wiley; 2006.
[23] Cortínez VH, Laura PAA. Further optimization of the Kantorovich method when applied to vibrations problems. Appl Acoust 1988;25:217–21.
[24] Oliva D, Hongisto V. Sound absorption of porous materials–accuracy of prediction methods. Appl Acoust 2013;74(12):1473–9.
[25] Delany ME, Bazley EN. Acoustical properties of fibrous absorbent materials. Appl Acoust 1970;3(2):105–16.
[26] Barron RF. Industrial noise control and acoustics. CRC Press; 2002.
[27] Kirkpatrick S, Gelatt CD, Vecchi MP. Optimization by simulated annealing. Science 1983;220:671–80.
[28] Petrowski JDA, Taillard PSE. Metaheuristics for hard optimization. Springer; 2006.
[29] Sonoflex SRL. Fonac – ECO (Polieter) <http://sonoflex.com/fonac/fonoabsorbente-conformado/>; [accessed 21.03.15].
[30] Bies DA, Hansen CH. Engineering noise control: theory and practice. CRC Press; 2009. p. 353–431.
[31] Wang CN, Torng JH. Experimental study of the absorption characteristics of some porous fibrous materials. Appl Acoust 2001;62(4):447–59.
[32] Keränen J, Airo E, Olkinuora P, Hongisto V. Validity of ray-tracing method for the application of noise control in workplaces. Acta Acust United Acust 2003;89(5):863–74.